International Journal of Radiation Oncology biology • physics

www.redjournal.org

Physics Contribution

Improving Tumor Treating Fields Treatment Efficacy in Patients With Glioblastoma Using Personalized Array Layouts

Cornelia Wenger, DrTechn,* Ricardo Salvador, PhD,* Peter J. Basser, PhD,† and Pedro C. Miranda, PhD*

**Institute of Biophysics and Biomedical Engineering, Faculdade de Ciências, Universidade de Lisboa, Lisbon, Portugal; and †Section on Tissue Biophysics and Biomimetics, Eunice Kennedy Shriver National Institute of Child Health and Human Development, National Institutes of Health, Bethesda, Maryland*

Received May 13, 2015, and in revised form Oct 12, 2015. Accepted for publication Nov 30, 2015.

Summary

Response to treatment with Tumor Treating Fields varies among glioblastoma patients. The field strength induced within the tumor is a crucial determinant for effective reduction in tumor growth. This computational study shows how the field delivery to the tumor can be optimized by specifically placing the transducer arrays in close proximity to the tumor.

Purpose: To investigate tumors of different size, shape, and location and the effect of varying transducer layouts on Tumor Treating Fields (TTFields) distribution in an anisotropic model.

Methods and Materials: A realistic human head model was generated from MR images of 1 healthy subject. Four different virtual tumors were placed at separate locations. The transducer arrays were modeled to mimic the TTFields-delivering commercial device. For each tumor location, varying array layouts were tested. The finite element method was used to calculate the electric field distribution, taking into account tissue heterogeneity and anisotropy.

Results: In all tumors, the average electric field induced by either of the 2 perpendicular array layouts exceeded the 1-V/cm therapeutic threshold value for TTFields effectiveness. Field strength within a tumor did not correlate with its size and shape but was higher in more superficial tumors. Additionally, it always increased when the array was adapted to the tumor's location. Compared with a default layout, the largest increase in field strength was 184%, and the highest average field strength induced in a tumor was 2.21 V/cm.

Conclusions: These results suggest that adapting array layouts to specific tumor locations can significantly increase field strength within the tumor. Our findings support the idea of personalized treatment planning to increase TTFields efficacy for patients with GBM.

Reprint requests to: Cornelia Wenger, DrTechn, Institute of Biophysics and Biomedical Engineering, Faculdade de Ciências, Campo Grande, Universidade de Lisboa, 1749-016 Lisboa, Portugal. Tel: (+351) 217-500-177; E-mail: cwenger@fc.ul.pt

C.W. and P.C.M. were supported by Novocure. P.J.B. was supported by the Intramural Research Program of the Eunice Kennedy Shriver National Institute of Child Health and Human Development, National Institutes of Health. P.C.M. and R.S. were supported in part by the Foundation for Science and Technology, Portugal.

Conflict of interest: none.

http://dx.doi.org/10.1016/j.ijrobp.2015.11.042

Introduction

Tumor Treating Fields (TTFields) are a novel antimitotic cancer treatment modality that disrupts cancer cell replication by applying alternating electric fields of low intensity (1-3 V/cm) and intermediate frequencies (100-300 kHz). The biological effects of TTFields were first observed during in vitro experiments, which showed a prolonged or completely arrested mitotic phase of treated cancer cells accompanied by membrane blebbing and rupture, often leading to cell death (1). The effect of TTFields is frequency-dependent; each cell line has a specific optimal frequency with maximal inhibitory effect on cell division (eg, 200 kHz for glioma cells) (2). TTFields are also dose-dependent; that is, the inhibitory effect of TTFields starts at 1 V/cm and increases with increasing field intensity (1, 2). After the antitumor effect of TTFields was demonstrated in animal tumor models (2), the Optune device (Novocure, Haifa, Israel), formerly known as the NovoTTF-100A system, was developed to deliver TTFields in human subjects with glioblastoma multiforme (GBM). In vitro experiments further showed that 2 perpendicular field directions were approximately 20% more effective than a single direction (2). Thus, clinically, TTFields are applied continuously by 2 pairs of transducer arrays, which are sequentially switched. Both pairs are placed on the patient's shaved scalp, one to the left and right (LR) of the tumor and one anterior and posterior (AP) to it (Fig. 1).

After encouraging results of a pilot trial in patients with recurrent GBM (2) indicating a favorable safety profile, a phase 3 trial (EF-11) compared TTFields therapy with physician's choice chemotherapy. The results showed similar efficacy between the 2 study arms, with no drug toxicity and better quality of life in TTFields-treated patients (3). Subsequently, the Patient Registry Dataset study (4), including 457 patients with recurrent GBM treated with Optune, showed significantly longer median overall survival with TTFields therapy in clinical practice (9.6 months) than in the EF-11 trial (6.6 months) and greater 1- and 2-year overall survival rates (1 year: 44% vs 20%; 2 years: 30% vs 9%). A recent phase 3 EF-14 trial comparing the combination of TTFields with temozolomide versus temozolomide alone in newly diagnosed GBM was terminated during interim analysis owing to early success of temozolomide with TTFields (5).

In all studies, response variability among patients was observed, which might be related to the efficacy of TTFields therapy being dose dependent. Because the field intensity cannot be measured inside the human head, computational modeling can be used as a proxy to estimate the induced electric field distribution. Previous studies showed that the field distribution is different for LR and AP pairs, and nonuniform, owing to tissue heterogeneity, with approximately 60% of the brain exposed to a field greater than 1 V/cm (6, 7). Furthermore, the average field in a virtual tumor at the same location in 2 different subjects showed ±25% variation about the mean value (8). This last study incorporated anisotropic conductivity tensors estimated using diffusion tensor imaging (DTI) data (9), because including white matter anisotropy was shown to substantially affect the electric field distribution in related techniques (10-13). Nonetheless, when including anisotropy for TTFields calculations, the field in the brain remained almost unchanged, and the average field strength in the tumor increased by 10% or less (8). A sensitivity analysis with reported ranges of conductivity and permittivity of head tissues showed a variation in field strength of

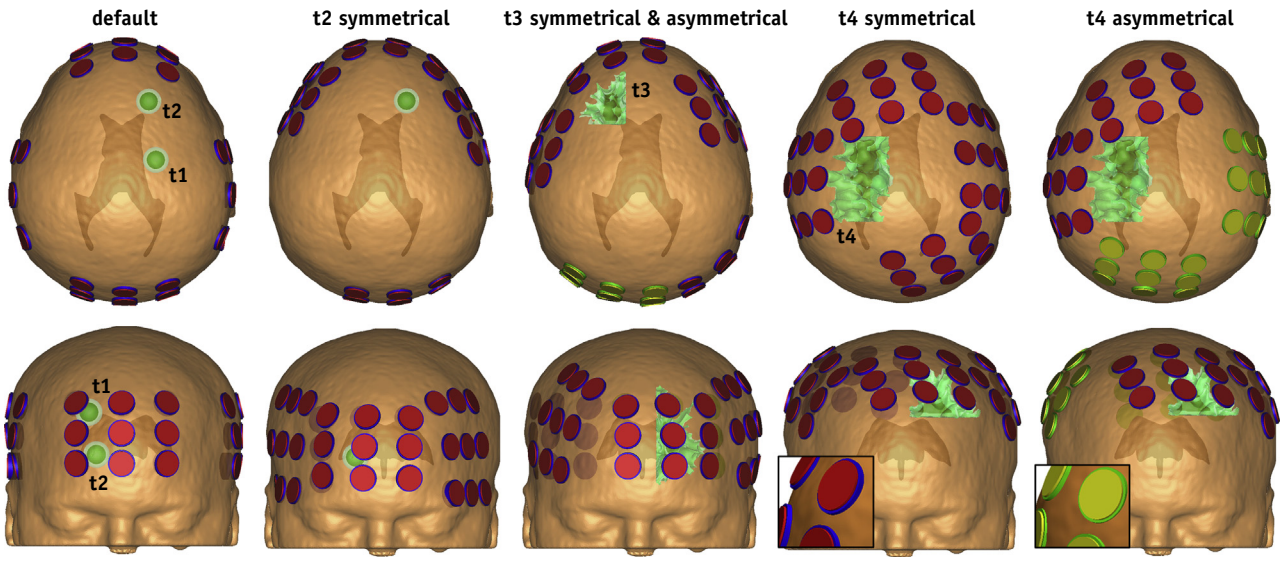

Fig. 1. Head model with scalp surface and ventricles. Tumors t1-t4 are presented in green. Top and front view of different layouts. Default and symmetric pads displayed in red/blue and asymmetric ones in yellow/green (insets). See main text for more details.

less than 42% in the brain and tumor (8). In all of these studies, only 1 tumor location and a single array layout were examined.

In this study we investigated tumors of different size, shape, and location and the effect of varying transducer layouts on TTFields distribution in an anisotropic model. We compared 2 spherical virtual tumors of equal size at different locations. Two larger, irregularly shaped tumors were also investigated. For the new tumor locations, we proposed adapted transducer layouts to improve field delivery to the tumor.

Methods and Materials

Creating the model

A realistic human head model was derived from MRI data of a healthy, young female subject, which consisted of T_1 and T_2 images with 1 × 1 × 1-mm^3 resolution. The MR images were segmented into scalp, skull, cerebrospinal fluid, gray matter (GM; including the cerebellum), white matter (WM), and ventricles. After registering the images to Montreal Neurological Institute space with FSL (14), the SimNibs pipeline (15) and the software package Brainsuite (16) were used to obtain each tissue surface.

The 4 virtual tumors were modeled within Mimics (Materialise, Leuven, Belgium) (Fig. 1). All consisted of a necrotic core and an active tumor shell with different dielectric properties (Table 1). As previously described (6) spherical tumor, t1, was placed in the right hemisphere near a lateral ventricle. The second tumor, t2, was an equally sized sphere, but shifted to a more anterior and inferior location. Both tumors t1 and t2 were represented by 2 concentric spheres, with core and shell volumes of 1.4 cm^3 and 2.8 cm^3, respectively. Two irregularly shaped tumors, t3 and t4, were also created. Tumor t3 was placed in the left anterior cingulate cortex, extending into the prefrontal cortex, with a shell volume of 13.9 cm^3 and a core volume of 2.8 cm^3. Tumor t4 was larger, with a shell volume of 22.8 cm^3 and a core volume of 3.8 cm^3, and was also placed in the left hemisphere, but more superficial and in the posterior frontal lobe, reaching the parietal lobe.

Table 1 Dielectric tissue properties at 200 kHz

Parameter	Conductivity, σ (S/m)	Relative permittivity, ε_r
Head		
Scalp	0.25	5000
Skull	0.013	200
Cerebrospinal fluid	1.79	110
Gray matter	0.25	3000
White matter	0.12	2000
Tumor		
Shell	0.24	2000
Core	1.00	110
Array		
Gel	0.10	100
Transducer	0	10,000

Each transducer array consisted of 3 × 3 transducers separated by 22 mm in one dimension and 33 mm in the other, representing the Optune system. A thin gel layer (0.5-2 mm) of 10-mm diameter was placed underneath each transducer, consisting of a 1-mm-thick ceramic disc, 9 mm in diameter. The default layout represents a symmetric configuration of LR and AP arrays (Fig. 1, left). This layout was applied to all tumors. For tumor locations other than for central t1, the array layouts were adapted to place them as close as possible to the tumor, taking into account space constraints. A second layout was created for t2, and 2 more were created for t3 and t4 (Fig. 1). For t3, only the back array of the AP setup differs between the 2 layouts: the asymmetric one is indicated by the yellow and green discs and the symmetric one by the blue and red discs (insets in Fig. 1). For t4, the right array of the LR pair was adapted to model a second asymmetric layout. Mimics was used to assemble all surface meshes into a volume mesh.

Solving the model

The electric field distribution within the brain was calculated using the finite element method to solve the quasi-static approximation of the Maxwell's equations, which is valid for this model (17). We used the Electric Currents Interface of COMSOL Multiphysics simulation software, which solves a current conservation problem for the scalar electric potential *V*. The chosen boundary conditions assume continuity of the normal component of the current density in all interior boundaries and electric insulation at the external boundaries. At each active transducer, a variable electrical potential was set at that boundary so that the integral of the current density normal to it is equal to 100 mA. The values of the heterogeneous dielectric properties were estimated specifically for 200 kHz, following a previous study (6) (Table 1).

The FSL diffusion toolbox (18) was used to correct and register the DTI images and calculate the eigenvectors, eigenvalues, and fractional anisotropy. Subsequently, the SimNibs MATLAB scripts (15) were used to estimate the conductivity tensors with baseline conductivity of the WM and the GM (Table 1). We used the volume normalized approach (19), whereby the geometric means of the eigenvalues of the conductivity tensor in each voxel are matched locally to isotropic reference values.

Results

All tumors and transducer layouts were evaluated. The average electric field strength was calculated in the brain, tumor shell (Table 2), and core. For tumor shells t2-t4, the values always increased for adapted array layouts (Table 2). In the necrotic core, the average field was always lower

Table 2 Average electric field strengths (V/cm) in all tumor shells for different array layouts

	LR				AP			
Tumor	Default	sym	asym	Max (sym, asym) default	Default	sym	asym	max(sym,asym)/default
t1	1.68				1.15			
t2	1.10	2.03		184%	2.08	2.21		107%
t3	1.10	1.76	1.76	161%	1.75	1.94	1.95	111%
t4	1.56	2.03	2.03	131%	1.20	1.46	1.61	134%

Abbreviations: AP = anterior-posterior; asym = asymmetric; LR = left-right; sym = symmetric.

than in the active shell. For a given tumor and stimulation direction, the ratio between average field in the shell and core was similar for all layouts.

The percentage of the tumor shell's volume having a field strength higher than 1, 2, or 3 V/cm was calculated. These above-threshold volumes (ATVs) will be referred to as ATV1, ATV2, and ATV3, respectively. The ATVs also increased for adapted array layouts (Table 3). The ATVs were evaluated separately for LR and AP setups, and for combined treatment (ie, the values in the LR*AP column of Table 3 represent the tumor shell's volume with a field strength above a certain value in both setups). Only maximum ATV values are presented, which for tumors t2-t4 originated from the adapted layouts. For tumors t3 and t4, the highest ATVs were achieved either for the symmetric or asymmetric layout, as noted in Table 3. The increase of ATVs compared with the values obtained with the default layout varied among tumors and setups (values in parentheses in Table 3). The highest increase of 48 percentage points was observed for the ATV2 of t2 under LR stimulation. In this case, the default layout induced a field greater than 2 V/cm in only 1% of the tumor shell, whereas for the adapted LR arrays, the ATV2 was 49%.

Figure 2 shows a comparison of the electric field distribution in axial slices through t3 induced by the default (middle) and the symmetric layout (bottom). The field is displayed only in the GM, WM, and tumor. The default LR setup was too central to have a strong effect on the frontal tumor (ie, the field was highest near the posterior limb of the internal capsule, close to the occipital horn of the lateral ventricle). When the LR array was adapted, the "hotspots" were shifted to the anterior limb of the internal capsule, close to the frontal horn of the lateral ventricle, resulting in additional hotspots at the interface with the tumor. The tumor's proximity to the anterior array induced high average fields within the tumor shell for default and adapted AP setups (Table 2). The strongest field appeared at the interface with the tumor, in the frontal forceps, and in the genu of the corpus callosum.

In the largest tumor, t4, the default layout produced average field strengths comparable to those in t1 (Table 2). However, by raising the transducer arrays closer to the higher tumor location, field strengths were increased, and hotspots were shifted from the temporal to the parietal lobe. Figure 3 illustrates the difference in the induced field distribution in t4 when the asymmetric layout is used instead of the default one. The stronger field produced by the asymmetric layout in the higher regions of the brain in the genu of internal capsule was clearly visible in the coronal and sagittal slices.

Discussion

In this study we examined tumors of different shape, size, and location, and we investigate whether array placement may influence TTFields efficacy. Tumor shape and size, up to 26.6 cm^3 total volume, did not have a noticeable impact on the average electric field strength in the tumor shell, owing primarily to the large size of the individual arrays.

Table 3 Largest ATVs in all tumor shells for LR and AP setups separately and for combined treatment (LR*AP)

	ATV1			ATV2			ATV3		
Tumor	LR	AP	LR*AP	LR	AP	LR*AP	LR	AP	LR*AP
t1	90%	58%	53%	23%	2%	0%	4%	0%	0%
t2	99%	100%	97%	49%	50%	22%	8%	17%	0%
	(+41%)*	(+0%)*	(+43%)*	(+48%)*	(+5%)*	(+21%)*	(+8%)*	(+5%)*	(+0%)*
t3	99%	100%	98%	25%	36%	6%	1%	4%	0%
	(+43%)†	(+1%)†	(+44%)†	(+24%)†	(+14%)*	(+6%)*	(+1%)*	(+3%)†	(+0%)†
t4	100%	100%	100%	51%	8%	2%	2%	0%	0%
	(+3%)†	(+11%)*	(+14%)*	(+38%)†	(+7%)*	(+2%)*	(+2%)†	(+0%)*	(+0%)†

Abbreviation: ATV = above-threshold volume. Other abbreviations as in Table 2.
The increase in percentage points compared with the default layout is given in parentheses.
* Values originated from the asymmetric layout.
† Values originated from the symmetric layout.

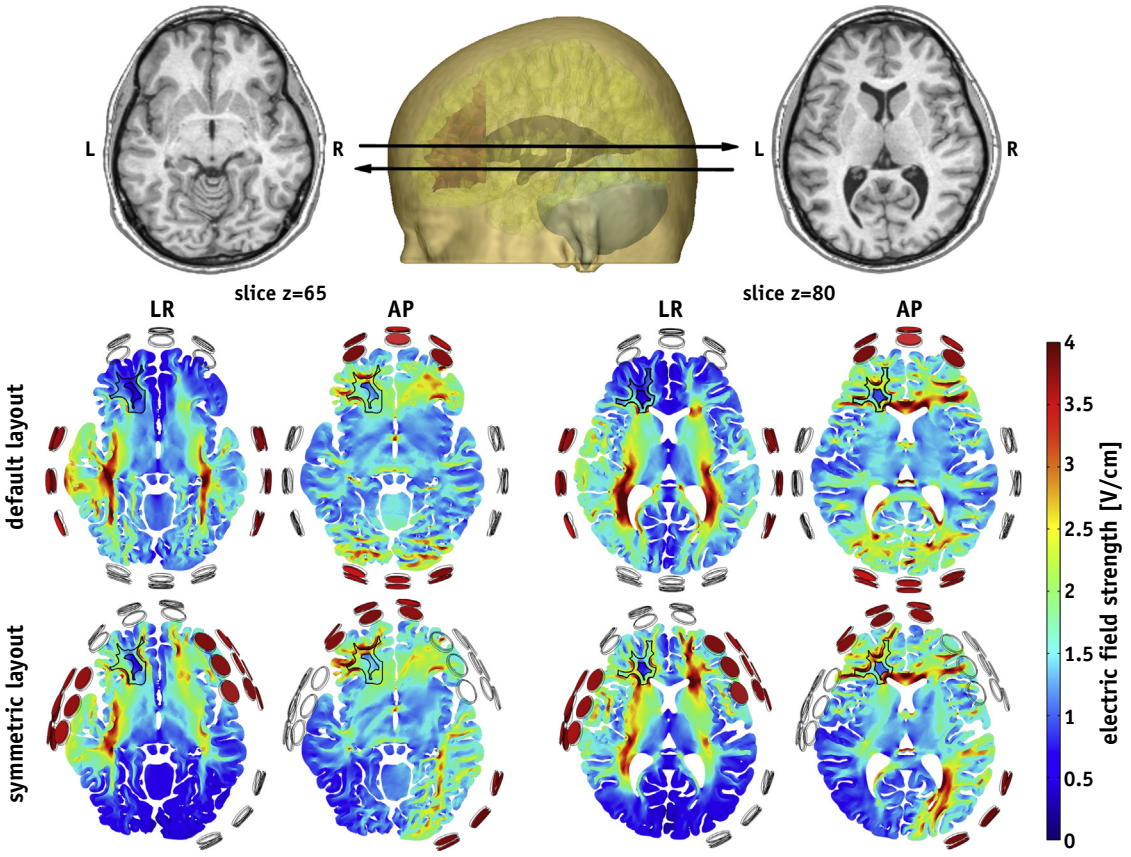

Fig. 2. Electric field distribution in 2 axial slices through t3 (contour shown in the left hemisphere, anteriorly). Default and symmetric layouts are presented for left-right (LR) and anterior-posterior (AP) setups. Corresponding anatomic slices and their position in the head model are presented at the top.

Thus, we focused on finding more effective transducer layouts, quantifying the difference in the average field strength within the tumor, and determining whether the ATVs can be enlarged.

The NovoTal system (Novocure) is approved in the United States to produce a personalized transducer array layout to maximize the intensity of TTFields within the tumor on the basis of morphologic measurements of the head, tumor size, and location(s) (20). Our assumptions for placing the adapted arrays are similar, because they were placed as close as possible to the tumor, taking into account space and anatomic constraints. Because this method does not yield one single layout, 2 possible layouts were compared for the irregular tumors. The results predict that by adapting the layout, the average field strength in the tumor would always increase. Yet, this increase varies: the smallest increase of 107% was present for t2 with the AP array, whereas the largest increase of 184% was predicted also for t2, but under LR stimulation (Table 2). Nonetheless, for all array configurations, including the default, the average field strength within all tumor shells exceeded the therapeutic threshold of 1 V/cm (Table 2). The highest average field of 2.21 V/cm appeared in the shell of t2 under adapted AP stimulation (Table 2). Apart from this maximum, the average field strength in the shell seemed to be close to or higher than 2 V/cm in many cases (eg, t2 with adapted LR arrays, t3 with adapted AP arrays, and t4 with adapted LR arrays). This increased field strength is crucial for treatment efficacy, because in vitro experiments predict a significant reduction in treated cell number when the field intensity is raised from 1 to 2 V/cm (1, 2) (eg, for rat glioma cells complete proliferation arrest has been seen after a 24-hour exposure to TTFields of 2.25 V/cm [1]).

For tumors t3 and t4, the increases for the symmetric and asymmetric setups were quite similar. Only for the AP stimulation of t4 was there a noticeable difference between the 2 adapted layouts, from 1.46 to 1.61 V/cm in the shell. These results indicate that the location of some arrays could be changed during treatment without losing efficacy. This might be of interest for the 16% of patients (3) who showed mild-to-moderate contact dermatitis underneath the transducers.

Depending on tumor location, either the LR or the AP array is more effective. Our findings suggest that for tumors located close to the central coronal plane, the LR setup produces stronger fields, whereas for tumors that are either more anterior or posterior, the AP setup is more effective.

Efficacy is also characterized by the evaluated ATVs. The ATV1 values correspond to the percentage of tumor shell exposed to fields higher than the therapeutic threshold

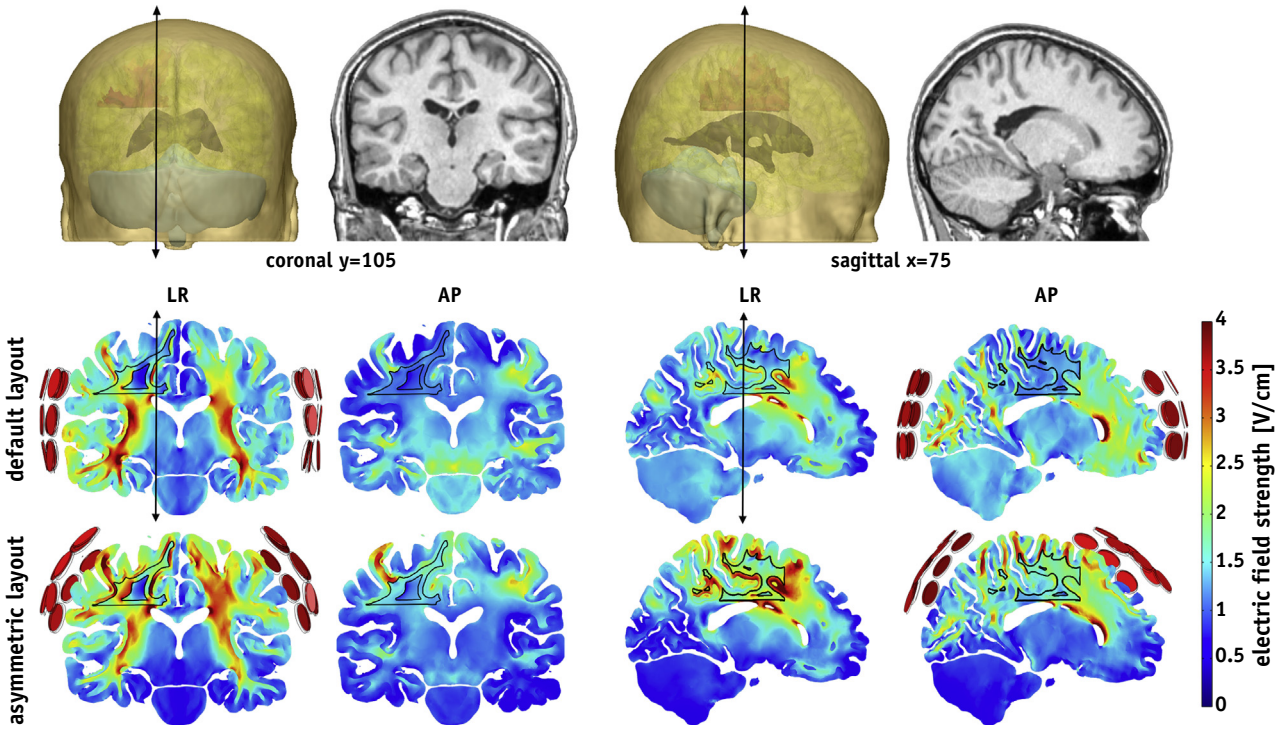

Fig. 3. Electric field distribution in a coronal and a sagittal slice through t4 (contour shown in the left hemisphere, above the ventricles). Default and asymmetric layouts are presented for left-right (LR) and anterior-posterior (AP) setups. Corresponding anatomic slices and their position in the head model are presented at the top.

value for TTFields therapy. Although for t1 the ATV1 was 90% for the LR array, it was reduced to 58% for the AP array, and only 53% for combined treatment. Thus, this central tumor is the most difficult to treat, where an adaption of the default layout, which cannot be placed closer to the tumor, will not lead to improvement. In all other tumors, the adapted layouts led to >97% exposure of the tumor shell to fields higher than 1 V/cm for combined treatment. Results show that TTFields may be most effective for t2: ATV2 values for both arrays were approximately 50% and 22% for LR*AP, and the ATV3 for the adapted AP arrays is 17%. The increased efficacy of TTFields by adapting layouts is shown in Table 3. Some ATVs are more than 40% higher when compared with the default layout (eg, the ATV1 induced by the LR array and LR*AP of tumors t2 and t3 and the ATV2 of t2 for the LR array). Furthermore, only for the adapted layouts the ATV2 values for combined treatment are nonzero for all tumors.

For the default layout the average electric fields in the brain were $E^{LR} = 1.45$ V/cm and $E^{AP} = 1.48$ V/cm. Despite the fact that these values and corresponding specific absorption rates are quite high, only limited adverse effects were reported in TTFields patients, as discussed in more detail elsewhere (6, 8). In all other array layouts, the average field strengths in the brain were lower. The lowest average field within the brain of 1.22 V/cm was induced by the adapted LR array for t2 and in the AP arrays of both adapted layouts for t4. Thus, apart from increasing the field within the tumor, adapting layouts decreases the field exposure of healthy tissues. This could also be the reason for the "out-of-field" recurrences observed in a recent study involving GBM patients treated with TTFields (21). In their report, the authors assumed that when the field is optimized in one direction, the field strength decreases elsewhere, where newly seeded tumor cells would be able to divide. The specific field distribution induced in the brain for t3 showed much lower field strength in the parietal area, which would correlate with recurrences observed in 2 patients in their study. The authors concluded that adjustment of arrays may lead to better response for locally progressing tumors. For multifocal diseases it might be justified to cycle through different layouts during earlier stages of treatment.

In summary, computational modeling is a practical means to analyze induced field distribution during TTFields treatment and to investigate factors that influence the field strength in the tumor. Previous studies focused on analyzing effects of including anisotropy of the WM, changing dielectric tissue properties and on intersubject variability (8). One limitation of all models, including the one presented here, is that local changes in tumor conductivity that might seem to be due to morphologic alterations, such as cell blebbing and rupture, are not accounted for. Indeed, it has been shown that the conductivity of the tumor has the strongest influence on the electric field in the tumor itself (8). An uncertainty in predicted average fields in the tumor shell of approximately ±33% was evaluated for conductivity values reported in literature. As already proposed (8), one way to address this limitation is to

acquire MRI and DTI data in patients. This additional information about the conductivity of tumor tissues and edematous areas can then be incorporated into realistic computational head models of patients.

Conclusion

The results of our finite element method computational model indicate that the average electric field induced by TTFields therapy was above the therapeutic threshold value of 1 V/cm in a variety of GBM tumors with different sizes, shapes, and locations. Furthermore, adapting transducer array layouts to specific tumor locations was highly beneficial, because it led to substantial increases in the induced field strength within the tumor and better TTFields coverage in the affected areas.

References

1. Kirson ED, Gurvich Z, Schneiderman R, et al. Disruption of cancer cell replication by alternating electric fields. *Cancer Res* 2004;64:3288-3295.
2. Kirson ED, Dbalý V, Tovarys F, et al. Alternating electric fields arrest cell proliferation in animal tumor models and human brain tumors. *Proc Natl Acad Sci U S A* 2007;104:10152-10157.
3. Stupp R, Wong ET, Kanner A, et al. NovoTTF-100A versus physician's choice chemotherapy in recurrent glioblastoma: A randomised phase III trial of a novel treatment modality. *Eur J Cancer* 2012;48:2192-2202.
4. Mrugala MM, Engelhard HH, Tran DD, et al. Clinical practice experience with NovoTTF-100A system for glioblastoma: The patient registry dataset (PRiDe). *Semin Oncol* 2014;41:S4-S13.
5. Stupp R, Wong ET, Scott CB, et al. NT-40 Interim analysis of the EF-14 trial: A prospective, multi-center trial of NovoTTF-100A together with temozolomide compared to temozolomide alone in patients with newly diagnosed GBM. *Neuro-Oncology* 2014;16:v167.
6. Miranda PC, Mekonnen A, Salvador R, et al. Predicting the electric field distribution in the brain for the treatment of glioblastoma. *Phys Med Biol* 2014;59:4137-4147.
7. Wenger C, Miranda PC, Mekonnen A, et al. Electric fields for the treatment of glioblastomas: A modeling study. *Neuro-Oncology* 2013;15(Suppl 3):iii235-iii241.
8. Wenger C, Salvador R, Basser PJ, et al. The electric field distribution in the brain during TTFields therapy and its dependence on tissue dielectric properties and anatomy: A computational study. *Phys Med Biol* 2015;60:7339-7357.
9. Basser PJ, Mattiello J, LeBihan D. MR diffusion tensor spectroscopy and imaging. *Biophys J* 1994;66:259-267.
10. Shahid S, Wen P, Ahfock T. Numerical investigation of white matter anisotropic conductivity in defining current distribution under tDCS. *Comput Methods Programs Biomed* 2013;109:48-64.
11. Shahid S, Wen P, Ahfock T. Assessment of electric field distribution in anisotropic cortical and subcortical regions under the influence of tDCS. *Bioelectromagnetics* 2014;57:41-57.
12. Suh HS, Lee WH, Kim T. Influence of anisotropic conductivity in the skull and white matter on transcranial direct current stimulation via an anatomically realistic finite element head model. *Phys Med Biol* 2012;57:6961.
13. Lee WH, Deng ZD, Laine AF, et al. Influence of white matter conductivity anisotropy on electric field strength induced by electroconvulsive therapy. *Conf Proc IEEE Eng Med Biol Soc* 2011;2011:5473-5476.
14. Jenkinson M, Beckmann CF, Behrens TEJ, et al. FSL. *Neuroimage* 2012;62:782-790.
15. Windhoff M, Opitz A, Thielscher A. Electric field calculations in brain stimulation based on finite elements: An optimized processing pipeline for the generation and usage of accurate individual head models. *Hum Brain Mapp* 2013;34:923-935.
16. Shattuck DW, Leahy RM. BrainSuite: An automated cortical surface identification tool. *Med Image Anal* 2002;6:129-142.
17. Haus HA, Melcher JR. Electromagnetic Fields and Energy. Cambridge, MA: Massachusetts Institute of Technology OpenCourseWare; 1989.
18. Smith SM, Jenkinson M, Woolrich MW, et al. Advances in functional and structural MR image analysis and implementation as FSL. *Neuroimage* 2004;23:208-219.
19. Güllmar D, Haueisen J, Reichenbach JR. Influence of anisotropic electrical conductivity in white matter tissue on the EEG/MEG forward and inverse solution. A high-resolution whole head simulation study. *Neuroimage* 2010;51:145-163.
20. Chaudhry A, Benson L, Varshaver M, et al. NovoTTF™-100A System (Tumor Treating Fields) transducer array layout planning for recurrent glioblastoma: A NovoTAL™ system user study. *World J Surg Oncol* 2015;13:316.
21. Turner SG, Gergel T, Wu H, et al. The effect of field strength on glioblastoma multiforme response in patients treated with the NovoTTF-100A system. *World J Surg Oncol* 2014;12:162.